Since January 2020 Elsevier has created a COVID-19 resource centre with free information in English and Mandarin on the novel coronavirus COVID-19. The COVID-19 resource centre is hosted on Elsevier Connect, the company's public news and information website.

Hygiene and Environmental Health Advances 3 (2022) 100015

Contents lists available at ScienceDirect

Hygiene and Environmental Health Advances

journal homepage: www.elsevier.com/locate/heha

Analysis of the spread of cough droplets and body deposition fraction in the smart classroom in different seasons

Mengfan Jia[a,b], Dan Mei[a,*], Jiaqian Li[a], Zihan Liu[a,c], Wenzhu Duan[a], Shanshan Hou[a,b]

[a] College of Resources and Environmental Engineering, Wuhan University of Science and Technology, Wuhan, 430081, Hubei, China
[b] School of Mechanical &Automotive Engineering, South China University of Technology, Guangzhou, 510641, Guangdong, China
[c] Northeastern University School of Resources and Civil Engineering, Northeastern University, Shenyang, 110819, Liaoning, China

ARTICLE INFO

Keywords:
Droplet transmission
Transmission distance
Exhaled height
Body deposition fraction

ABSTRACT

Smart classrooms are a relatively confined public space for college students. SARS-COV-2 and other respiratory viruses have been shown to pose a more significant threat to human health in relatively confined spaces. Using numerical simulation method to simulate the transmission and concentration distribution of virus-carrying droplets in smart classrooms in three different seasons (summer, winter, transitional seasons: spring and autumn). The Realizable k-ε model is used to simulate the airflow pattern in the smart classroom, and the Lagrangian method is used to simulate the transmission of droplets. The transmission process of droplets produced from the teacher standing on the platform and the student sitting on the seat is studied. The influence of three kinds of outdoor temperature on droplet transmission and the body deposition fraction of people in the smart classroom is analyzed. The results show that droplet transmission speed is maximum at the temperature of 5 degrees when the outdoor temperature is 5 °C, 20 °C, and 35 °C respectively. At 10 s, the transmission distance of droplets increases by 9.55% compared with that at 20 °C and 10.31% compared with that at 35 °C. In addition, the body deposition fraction is also affected by the location of the vent, with downwind contact being 6 times more likely than upwind contact. The research results can provide suggestions and measures for epidemic prevention and control in smart classrooms.

1. Introduction

Infectious respiratory diseases such as influenza, tuberculosis, and severe acute respiratory syndrome (SARS) have threatened human health for nearly two decades. In 2019, the Novel Coronavirus (SARS-COV-2) spread worldwide, causing a global emergency (World Health Organization 2020a, World Health Organization 2020b). Regarding physical properties, viruses are ultrafine particles attached to dust or other carriers. Theoretically predict the movement and transmission laws of the droplets in the air (Liu, 2007), and provide a sufficient basis for the effective prevention and control of the spread of diseases. Therefore, raising awareness of virus-carrying droplet transmission is very important for understanding respiratory diseases such as SARS-COV-2 and influenza (Zhang et al., 2019, G et al., 2015).

At present, there are three main research methods on droplet transmission characteristics at home and abroad: theoretical analysis, experimental research, and numerical simulation (Zhao, 2006). Research focuses on droplet transmission mechanisms, factors affecting airflow, droplet transmission in different scenarios, etc. In the study of droplets movement and transmission discipline, many numerical simulation methods are used because the experimental research method is time-consuming, expensive, and dangerous (such as SARS-COV-2) and so on. The numerical simulation method has the advantages of low cost, fast calculation speed, comparison of various working conditions and benchmark experiment verification, and high reliability (Zhao, 2006, Wang, Zhang & Wang, 2007).

In indoor environments, droplets produced by the respiratory system may carry pathogens that have the opportunity to spread through the air and invade new hosts (Li et al., 2018). In a relatively confined environment exposed to high concentrations of aerosols for a long time, there is a possibility of aerosol transmission (National Health Commission of the People's Republic of China 2021), which will increase the risk of infection (Yu et al., 2020, Carrillo, Rodríguez & Aranaga, 2019). With the development of smart education, smart classrooms are gradually popularized in universities (Wang & Yao, 2020). In the smart classroom, students sit face to face at the same table, and the smart classroom is a relatively confined space that adopts mechanical ventilation. In other words, the distance between people in the classroom is shortened, thus increasing the chance of droplets being inhaled and contacted, increasing the risk of infection (Kang et al., 2015). In relatively confined environments,

* Corresponding author:
E-mail address: meidan@wust.edu.cn (D. Mei).

https://doi.org/10.1016/j.heha.2022.100015
Received 22 April 2022; Received in revised form 24 June 2022; Accepted 25 June 2022

droplets exhaled by different respiratory activities can carry infectious viruses, which evaporate, spread, suspend in the air or lodge on walls, and then are inhaled, creating a potential infection risk (G et al., 2015, Wang, Zhang & Wang, 2007, Gao, Niu & Morawska, 2010, Zhang et al., 2017, Hang, Li & Jin, 2014). Therefore, it is necessary to study the transmission of droplets in the relatively confined smart classroom.

Some researchers used the computational fluid dynamics (CFD) simulation method to study the evaporation and migration process of solid-liquid mixed droplets with different initial diameters exhaled in a passenger car (Yang, Yang & Zhao, 2016, Chao & Wan, 2006). They simulated their experimental cases and compared the data, which showed the vertical position trajectory of droplets in Yang et al. (Yang, Yang & Zhao, 2016)is in good agreement with the experimental results. Many studies have also demonstrated the accuracy of numerical simulations in droplet transport (Cai, 2019), indoor airflow organization (Gao, 2014, Wei, 2007), etc. Therefore, the method of numerical simulation is selected in the research of this article.

At present, the research on the droplet transmission process mainly focuses on the kinetic characteristics of droplets, the particle size of droplets, temperature, and humidity. Liu (Liu, 2007) has conducted an in-depth analysis of the stress of microbial aerosols. In the process of transmission, its movement is affected by gravity, drag, thermophoresis, Saffman force, Brownian force, and other forces. Meanwhile, due to its characteristics, droplet transmission is accompanied by evaporation, attenuation, settlement, and other dynamic factors, which in turn affect its transmission characteristics (Liu, 2007, Kang, Zhang & Feng, 2017). Chen and Zhao (Chen & Zhao, 2010)'s research results show that the influence of temperature and relative humidity on droplet dispersion is negligible for droplets with an initial diameter of fewer than 200 μm. Wang (Wang, 2011) analyzed the airborne transmission process of respiratory diseases through droplets and droplet nuclei..and found that the deposition rate and evaporation rate of droplets decreased with decreasing droplet size. It can be seen from the above research that the influence of temperature and relative humidity on the dispersion of cough droplets can be ignored.

Taking the relatively confined smart classroom as the research object, the transmission and concentration distribution of virus-carrying droplets in the smart classroom in different seasons were simulated by FLUENT software. The transmission of droplets from a cough of one person at a table under the podium in the smart classroom was studied and the body deposition fraction of each person at the table was assessed. Studies on the transmission process of droplets in smart classrooms under these two scenarios and the assessment of the fraction of body deposition can provide some reference opinions for preventing and controlling COVID-19 in smart classrooms.

2. Method

2.1. Geometric model and case design

A smart classroom with a size of 15 m × 8 m × 3 m (X × Z × Y) was used to study the influence of different outdoor temperatures on the spread of indoor droplets, and a body deposition fraction assessment was conducted for people sitting at different positions of the desk. The air conditioner is located above the suspended ceiling, the air outlet size is 0.95 m × 0.95 m (X × Z), and the door size is 2 m × 1 m (Y × X). More details of the room can be seen in Fig. 1 and Table 1. Two scenarios were studied: scenario 1 is shown in Fig. 1(a). There are only human bodies A, B, C, D, E, F, and G in the classroom. The red human body B is the source of infection, and the others are uninfected. Scene 2 is shown in Fig. 1(b). Teacher A on the podium is the source of disease, and the others are uninfected.

Zhang (Zhang, 2011)used numerical simulation to analyze the impact of environmental temperature changes on the transmission process of droplets, considering that whether it was the SARS outbreak in 2003 or the pandemic of influenza A in 2009, it all occurred in the spring and autumn. Season, not in the hot summer. In combination with reality, the environment temperature is 280K (7°C) and 298K (25°C) for simulation. The results show that the droplet transmission distance is longer when the ambient temperature is 280K. Seasonal signals decomposed by Ensemble Empirical Mode Decomposition showed that the infectivity and mortality of SARS-COV-2 were higher in a cold climate (Liu, Huang & Li, 2021). In these two scenarios, three different temperatures are set 5 °C, 35 °C, and 20 °C, representing winter, summer, and transition seasons (spring and autumn) respectively. Model validation sees supplementary material.

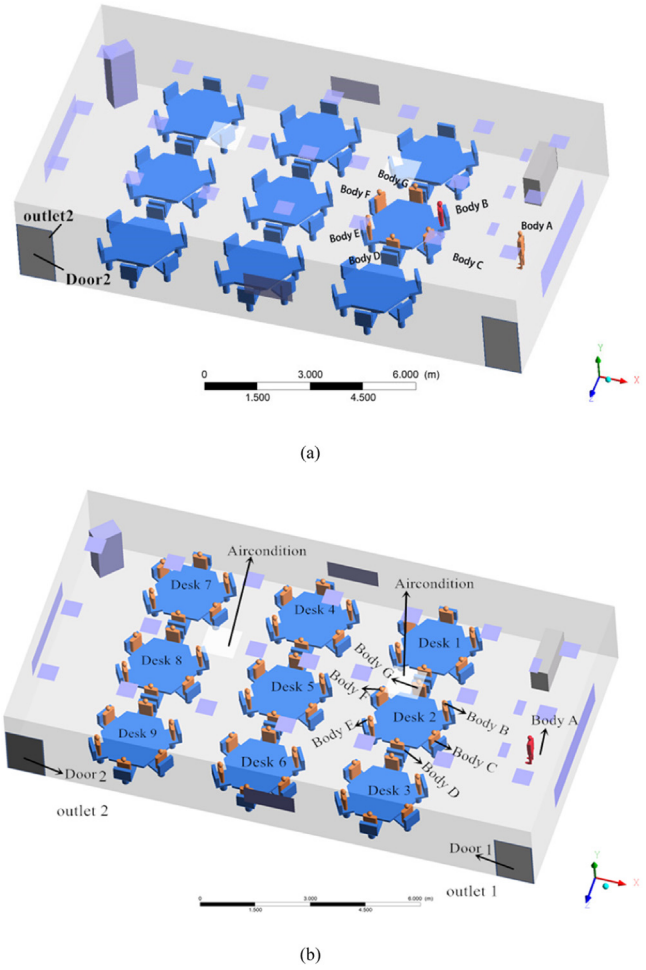

Fig. 1. The schematic of the simulated smart classroom

Table 1
Description of the simulated smart classroom.

Name	X/m	Y/m	Z/m	notes
Room	15	8	3	/
Seats	0.5	0.4	0.1	0.5 m from the ground, 2 m between two
Seatbacks	0.5	0.5	0.1	opposite seats at the same table
Platform	1.5	0.5	1	0.1 m from the left wall, 1.5 m from the back wall
air-conditioners	9.5	9.5	/	located on the top wall of the room
Door1/Door2	2	1	0.4	/
Lights	0.5	0.5	/	/

2.2. Meshing

The complex smart classroom model is divided by an unstructured grid. During the division, the grids of the human mouth, the speed entrance of the air conditioner, and the pressure exit of the door slit were

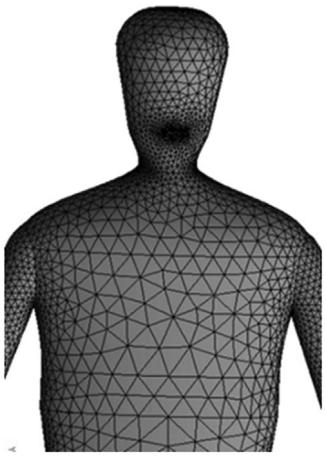

Fig. 2. Grid of the human body on the podium

encrypted, and the model was divided into different numbers of grids. The number of grids used in the two scenarios is 2.27 million and 3.26 million respectively. The encrypted human body grid is shown in Fig. 2. Mesh independence verification see supplementary material.

2.3. Physical model

2.3.1. Gas flow equations

Fluids are mainly divided into the laminar flow and turbulent flow. Turbulent flow is characterized by pulsating velocity field, which is primarily caused by velocity changes and appears where the velocity changes. For example, the flow of gases in the air generated during respiration is turbulent flow (Zhang, 2011). Due to a large number of people and the influence of air conditioning and other factors, the flow of air in the smart classroom is turbulent. The air is a Newtonian fluid, and the continuous flow is solved by the Reynolds average Navier-Stokes (RANS) equation, as shown below:

Continuity equation:

$$\frac{\partial u}{\partial x}+\frac{\partial v}{\partial y}+\frac{\partial w}{\partial z}=0 \tag{1}$$

Momentum equation:

X-axis:

$$\frac{\partial(\rho u)}{\partial t}+\frac{\partial(\rho uu)}{\partial x}+\frac{\partial(\rho uv)}{\partial y}+\frac{\partial(\rho uw)}{\partial z}=\frac{\partial}{\partial x}\left(\mu\frac{\partial u}{\partial x}\right)+\frac{\partial}{\partial y}\left(\mu\frac{\partial u}{\partial y}\right)+\frac{\partial}{\partial z}\left(\mu\frac{\partial u}{\partial z}\right)-\frac{\partial p}{\partial x} \tag{2}$$

Y-axis:

$$\frac{\partial(\rho v)}{\partial t}+\frac{\partial(\rho vu)}{\partial x}+\frac{\partial(\rho vv)}{\partial y}+\frac{\partial(\rho vw)}{\partial z}=\frac{\partial}{\partial x}\left(\mu\frac{\partial v}{\partial x}\right)+\frac{\partial}{\partial y}\left(\mu\frac{\partial v}{\partial y}\right)+\frac{\partial}{\partial z}\left(\mu\frac{\partial v}{\partial z}\right)-\frac{\partial p}{\partial x}-\rho g \tag{3}$$

Z-axis:

$$\frac{\partial(\rho w)}{\partial t}+\frac{\partial(\rho wu)}{\partial x}+\frac{\partial(\rho wv)}{\partial y}+\frac{\partial(\rho ww)}{\partial z}=\frac{\partial}{\partial x}\left(\mu\frac{\partial w}{\partial x}\right)+\frac{\partial}{\partial y}\left(\mu\frac{\partial w}{\partial y}\right)+\frac{\partial}{\partial z}\left(\mu\frac{\partial w}{\partial z}\right)-\frac{\partial p}{\partial x} \tag{4}$$

where g is the acceleration due to gravity, ρ is the fluid density, u is the average velocity of the fluid, and P is the fluid pressure; u, v, w are the velocity components of the fluid at a specific moment; the constant μ is the dynamic viscosity.

Energy equation:

$$\frac{\partial(\rho T)}{\partial t}+\frac{\partial(\rho uT)}{\partial x}+\frac{\partial(\rho vT)}{\partial y}+\frac{\partial(\rho wT)}{\partial z}=\frac{\partial}{\partial z}\left(\frac{k}{c_p}\frac{\partial T}{\partial x}\right)-\frac{\partial}{\partial y}\left(\frac{k}{c_p}\frac{\partial T}{\partial y}\right)+\frac{\partial}{\partial z}\left(\frac{k}{c_p}\frac{\partial T}{\partial z}\right)+S_T \tag{5}$$

where Cp is the specific heat capacity, T is the temperature (K), k is the heat transfer coefficient of the fluid, ST is the internal heat source of the fluid and the part where the fluid's mechanical energy is converted into thermal energy due to viscous action. In this study, the internal heat source is Heat generated by Lights, Body Surfaces, Screens, and Server.

Indoor airflow is generally turbulent [(Kang et al., 2015),Error! Bookmark not defined.]. The standard k-ε model has a relatively simple situation and is only suitable for simulating a completely turbulent flow process. For the simulation of indoor air distribution, the Realizable k-ε model is based on the standard k-ε model, which imposes certain mathematical constraints on the normal stress, reflecting the time-averaged strain rate, and its suitable flow types are relatively wide (Abdi & Bitsuamlak, 2014, Rahimi, Tavakoli & Zahiri, 2014). Therefore, the Realizable k-ε turbulence model is selected for the research.

The model transportation equation of k and ε in the achievable k-ε model is:

$$\frac{\partial}{\partial t}(\rho k)+\frac{\partial}{\partial x_j}(\rho k u_j)=\frac{\partial}{\partial x_j}\left[\left(\mu+\frac{\mu_t}{\sigma_k}\right)\frac{\partial k}{\partial x_j}\right]+G_k+G_b-\rho\varepsilon-Y_M \tag{6}$$

And

$$\frac{\partial}{\partial t}(\rho\varepsilon)+\frac{\partial}{\partial x_j}(\rho\varepsilon u_j)=\frac{\partial}{\partial x_j}\left[\left(\mu+\frac{\mu_t}{\sigma_\varepsilon}\right)\frac{\partial\varepsilon}{\partial x_j}\right]+\rho C_1 S\varepsilon-\rho C_2\frac{\varepsilon^2}{k+\sqrt{\upsilon\varepsilon}}+C_{1\varepsilon}\frac{\varepsilon}{k}C_{3\varepsilon}G_b \tag{7}$$

where $C_1=\max[0.43,\frac{\eta}{\eta+5}],\eta=S\frac{k}{\varepsilon},S=\sqrt{2S_{ij}S_{ij}}$.

In the above equation, G_k represents the turbulent kinetic energy due to the average velocity gradient, as described in the turbulence generation model in the k-ε model. G_b is the turbulent flow energy generated by buoyancy, which is calculated as described in the "Effect of Buoyancy on Turbulence" in the k-ε model. Y_M represents the contribution of fluctuating expansion incompressible turbulence to the total dissipation rate, as described in the influence of compressibility on turbulence in the k-ε model. C_2 and $C_{1\varepsilon}$ are constants. σ_k and σ_ε are the turbulent Prandtl numbers of turbulent kinetic energy k and dissipation rate ε, respectively.

2.3.2. Discrete Phase Transmission Model

Since the transmission of droplets in the air is discrete, the Lagrangian method is used to study the transmission process of droplets. The discrete phase model (DPM) in FLUENT assumes that the second phase (dispersed phase) is very thin, so particle-particle interactions and particle volume fraction effects on the continuous phase are not considered. Therefore, thermal swim force, Saffman force, and pressure gradient force were considered in this study. The Lagrangian equation describing the movement of droplets is (Wang, 2004):

$$\frac{dx_p}{dt}=u_p \tag{8}$$

$$\frac{du_p}{dt}=\frac{f_D}{\tau_p}(u-u_p)+F_p \tag{9}$$

where x_p is the moving distance, t is the time, and up is the speed of droplets. F_p stands for other external forces; this study considers Saffman's lift force, thermophoresis force, and pressure gradient force. f_D is Stokes drag modification function. For large droplets Reynolds number (Rep).

$$f_D(\mathrm{Re}_p)=1+0.15\mathrm{Re}_p^{0.687} \tag{10}$$

Table 2
Boundary conditions in airflow simulation.

Boundary name	Boundary conditions
Air-conditioners	velocity inlet, velocity is 0.66 $m{\cdot}s^{-1}$, the temperature is 20 °C
Mouth	velocity inlet, velocity is 22 $m{\cdot}s^{-1}$, the temperature is 36 °C, only the exhale of the respiratory system is considered
Outlet 1/ Outlet 2	pressure outlet
Body surface	standard wall function, no slip wall, heat flux is 26 $W{\cdot}m^{-2}$ for all the manikins
Left and right wall	standard wall function, no slip wall, heat transfer coefficient is 0.34 $W{\cdot}m^{-2}{\cdot}K^{-1}$) and temperature is same as outside
Back, bottom, front, and top wall	standard wall function, no-slip wall, heat flux is 0 $W{\cdot}m^{-2}$
Screens	heat flux is 46 $W{\cdot}m^{-2}$
Lights	heat flux is 28 $W{\cdot}m^{-2}$
Server	heat flux is 100 $W{\cdot}m^{-2}$

Droplets' characteristic time is defined as:

$$\tau_{\mathrm{p}} = \frac{\rho_p D_p^2 C_c}{18\mu} \tag{11}$$

The Cunningham slip correction factor Cc for tiny droplets in the formula is:

$$C_{\mathrm{c}} = 1 + \frac{2\lambda}{D_P}\left(1.257 + 0.4\exp\left(-\frac{1.1 D_p}{2\lambda}\right)\right) \tag{12}$$

D_p is the diameter of droplets, and λ is the free path.

2.4. Boundary conditions

The accuracy of CFD simulation results largely depends on the setting of boundary conditions. All boundary conditions are set as shown in Table 2.

The human body's cough time is 0.5 s (Carrillo, Rodríguez & Aranaga, 2019), so the spraying time of droplets is set to 0.5 s, and the speed is set to 22 $m{\cdot}s^{-1}$ (Deacon, 2001, Zhao, Zhang & Li, 2003), and the temperature of droplets is set to 36 °C (Gao, Niu & Morawska, 2010, He et al., 2011). The angle θ of the exhaled airflow from the source of infection (the angle between the center of the airflow and the horizontal line when viewed from the side) is taken as 19 ° (Zhu, Kato & Yang, 2006). The convective heat flow on the human body surface is 26 $W{\cdot}m^{-2}$.

Sneezing or coughing can produce a large number of droplets with a diameter of about 10-100 μm. However, they will split into droplets with a diameter of 1 μm in a very short time (Deacon, 2001, Zhao, Zhang & Li, 2003). And in the case of evaporation and condensation, droplets with an initial diameter of 10 μm will evaporate within the first 0.2 s (Yang et al., 2020). The smaller the particle size of droplets, the shorter the evaporation time of the virus-carrying droplets (Wang et al., 2020), so the time droplets are at a large particle size is very short and unstable. Therefore, the influence of evaporation on droplets is ignored during the simulation, and droplets size is assumed to be 1 μm (Yang et al., 2020, Liu, Zhang & Dan, 2016).

2.5. Body deposition fraction assessment

After the outbreak of the SARS-COV-2 epidemic, many studies have shown that the transmission of the SARS-COv-2 includes respiratory droplet transmission and close contact transmission. It can be transmitted by aerosols in a relatively confined environment, and it can also cause infection after contacting with virus-contaminated items. Some researchers also study the risk of infection through the amount of pathogen deposition (Health Commission website 2022, Nicas & Best, 2008). In the study of droplet transmission in the smart classroom, considering that droplets may be transmitted through contact if it falls on the human body, the body deposition fraction can be characterized by quantification of droplet deposition.

Studies have found that under normal temperature conditions, regardless of whether the SARS-COv-2 or SARS virus, it can only survive in the air for three hours (Sun, Huang & Zhang, 2020). It takes about three days for plastics to drop below the infectivity level. Ong et al.'s (Ong et al., 2020)research showed that nucleic acid could be detected on the surface of various objects in the patient's room. It can be seen that the deposited droplets still have a risk of contact, and it is feasible to judge the fraction of body deposition based on the amount of deposition. A simple body deposition fraction model was established based on it, where the fraction of body deposition P is defined as the ratio of the number of droplets deposited on each person to the total amount of droplets deposited, namely:

$$P_i = \frac{X_i}{Z} \tag{13}$$

In the formula, P_i represents the body deposition fraction of the uninfected person i, Z represents the total amount of droplets deposited, and X_i represents the number of droplets deposited on the uninfected person i.

3. Results and Discussion

3.1. Scenario 1: When the source of infection is sitting students, the fraction of body deposition of other personnel is assessed

3.1.1. The influence of environmental temperature on the spread of cough droplets

It can be seen from Fig. 3 that when t = 0.5 s, droplets coughed up by the infected person are distributed in cones. At 1 s, due to the vertical downward airflow, the impact of gravity and inertial force on droplets makes droplets deposited on the Desk 2 reach 87% of the total number of droplets. These droplets carrying infectious bacteria or viruses deposited on the desk will pose a potential threaten to people. At 1.5 s, due to the effect of air conditioning wind, droplets spread around. Because of the source of infection faces in the X- direction, with the impact of the droplets' inertia, the movement of droplets in the negative direction of the X direction is faster than the positive direction of the X direction. When t = 4.5 s, as droplets continue to spread, droplets have reached Desk 5. At this time, there are a large number of droplets around the susceptible person E, who is opposite to the source of infection B, and the number of droplets on the right side of the susceptible person E is much larger than the number of droplets on the left side. The main reason for this is that the air outlet is located on the right side of the susceptible person E, and the pressure on the right side of person E is lower than that on the left side. At 8.5 s, droplets have reached Desk 6, which gradually spread to Desk 6 after that. According to the trajectory of droplets within 10 s, the risk of droplets spreading to the Desk 6 is very high. In short, when the source of infection B coughs, the susceptible person E relative to the source of infection B has the highest body deposition fraction.

According to the difference between the coordinates of the location of the source of infection and the coordinates when the concentration of droplets becomes zero during the process of spreading to the surroundings, the transmission distance of droplets at different times can be obtained. The changes of droplets' transmission distance at different outdoor temperatures is shown in Fig. 4. It can be seen from Fig. 4 that no matter in which direction, under the same transmission time, the

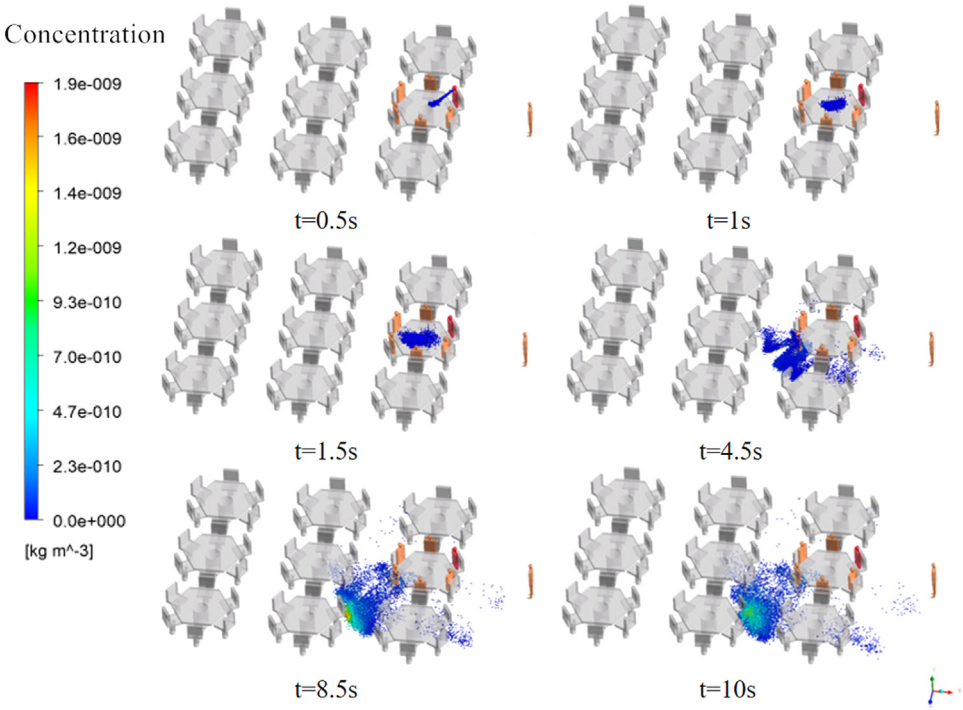

Fig. 3. The spread of droplets at different times when the temperature is 5 ℃

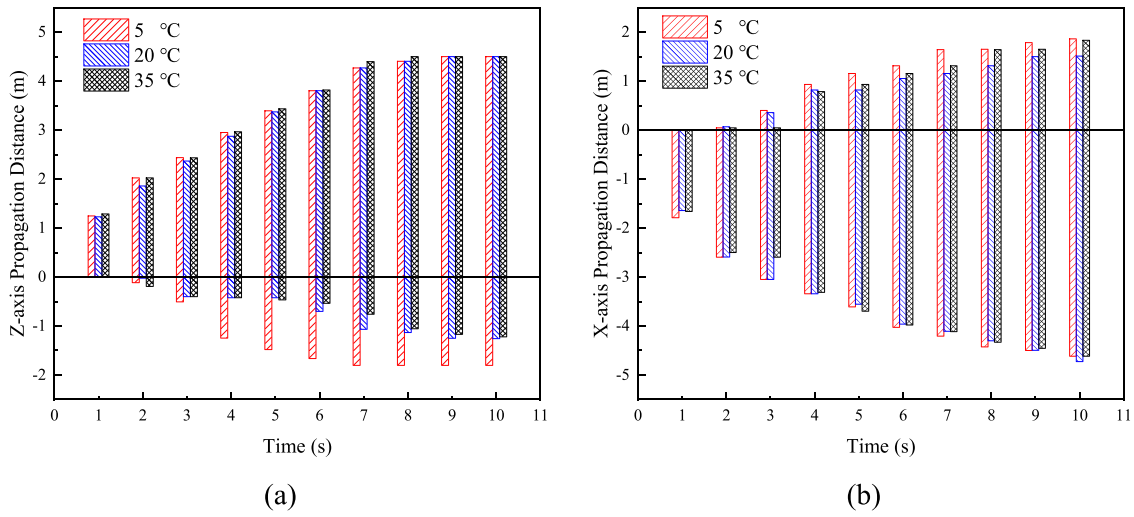

Fig. 4. The propagation distance of droplets in different directions at different moments (a)The propagation distance of droplets on the Z axis at different moments, Z+ means propagation to the left, Z+ means propagation to the right (b) The propagation distance of droplets on the X-axis at different times, X+ means backward propagation, X- means forward propagation

transmission distance of droplets is the largest when the outdoor temperature is 5 ℃ (winter). At the three temperatures of 5 ℃, 20 ℃, and 35 ℃, droplets have spread to the wall in the Z +direction at a distance of 4.50 m at 9 s, and the distance traveled in the Z-direction in the 5 ℃ direction is the farthest, 1.81 m. In the X+ direction within 10 s, the transmission distance is the farthest when the temperature is 5 ℃, and the transmission distance is 4.73 m. In the X- Direction, the transmission distance is the farthest when the temperature is 5 ℃, and the transmission distance is 1.86 m. When the temperature is 20 ℃, within 10 s, the farthest forward travel distance of droplets is 1.51 m, the backward 2.91 m, the left 4.50 m, and the right 1.26 m. When the temperature is 35 ℃, the farthest droplets' transmission distance can reach 4.62 m forward, 1.83 m backward, 4.50 m to the left, and 1.22 m to the right within 10 s. The main reason for the difference in droplets transmission in different directions is that the direction of the airflow of the exhaled droplets is along the X- Direction, so droplets transmission distance is the longest in the X- Direction at three different temperatures. In summary, at the three temperatures in this scene, the transmission distance of droplets can reach 1.22 m at the nearest and 4.73 m at the farthest in 10 s. The greater the temperature difference between indoor and outdoor, the greater the pressure difference, and the greater the airflow velocity. Therefore, the drop in temperature accelerates the spread of droplets. In different directions, when the outdoor temperature is 5 ℃, the spread of droplets is the farthest.

3.1.2. Evaluation of body deposition fraction of personnel in Desk 2

It can be seen from Fig. 5 that $P_E > P_D > P_C > P_F > P_G > P$, the susceptible person E has the highest body deposition fraction, followed by D, C, F, and G. The body deposition fraction of the susceptible person E is 173 times higher than that of susceptible person D, 1112 times higher

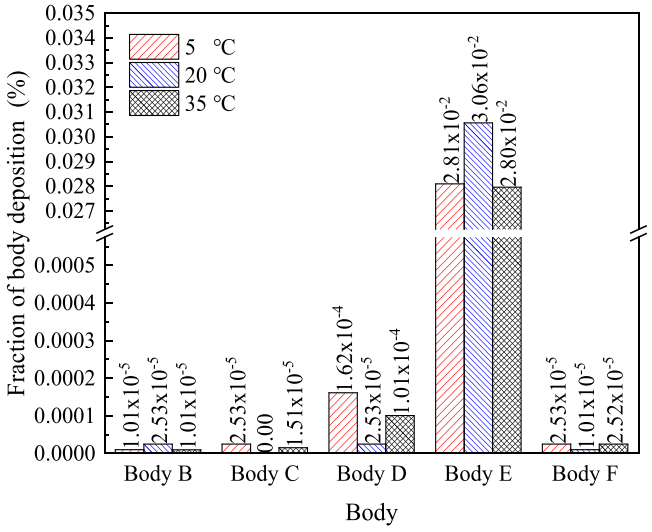

Fig. 5. Fraction of body deposition with different human bodies in 10 s

than that of susceptible person C, and 1112 times higher than that of susceptible person F. Susceptible person G has no droplets deposited. It can be seen from Fig. 4 that the susceptible person E located directly opposite the source of infection B has the highest body deposition fraction, followed by D, which is adjacent to the susceptible person E. It can be seen from Fig. 5 that it is not the susceptible person F adjacent to E that has the greater fraction of body deposition, but the susceptible person D. And susceptible person D is 6 times as susceptible person F. There is no droplets deposited on G adjacent to the source of infection B, while there are droplets deposit on C. This shows that when droplets on the Desk 2 are spreading, they will be affected by the position of the exhaust vent. The pressure at the exhaust vent is as small as -20 pa. And the vent is close to the human body C, so droplet deposits on the susceptible persons C and D are larger, and the body deposition fraction is also greater.

3.2. Scenario 2: When the source of infection is a teacher on the podium, evaluation of the body deposition fraction of other people

Another type of people who often use smart classrooms are teachers, who usually stand up to teach in smart classrooms. When the source of infection is the teacher on the podium, the position and exhaled height (The height of the middle position of the human mouth and nose from the ground) of the source of infection will change compared with the sitting student. Therefore, the scene where the source of infection is the teacher on the podium was studied, and the fraction of body deposition with other desks was also evaluated.

3.2.1. The influence of environmental temperature on the spread of cough droplets

It can be seen from Fig. 6 that at 0.5 s, droplets produced by coughing are distributed in a cone. Since the initial direction of the cough droplets is at an angle of 19 ° to the horizontal plane, droplets are mainly affected by the inertial force and propagate obliquely downwards. At 2 s, droplets gradually spread to the surroundings. At 4 s, droplets had reached the edge of Desk 2. At this time, the cough droplets reached the ground and spread further. At 8 s, droplets have spread to Desk 3. At 13 s and 15 s, it can be seen that droplet distribution has not changed much. At this time, almost no droplets were found near Desk 1.

The teacher on the podium is located in the horizontal middle of the smart classroom model. It can be seen from Fig. 6 that the cough droplets tend to spread to Desk 2 and transition to Desk 3. However, there are few droplets in the direction of Desk 1, and they are not evenly distributed on both sides. It can be concluded that the direction of the pressure outlet will affect the direction of droplet diffusion, so three cross-sections were made to verify this hypothesis, as shown in Fig. 7.

It can be seen from Fig. 8 that the speed above Desk 3 is higher than that of Desk 1. The speed of Desk 3 reaches 0.16 $m{\cdot}s^{-1}$. The flow velocity above Desk 1 is 0.07 $m{\cdot}s^{-1}$, and a vortex is formed. When there are pollutants in the room, due to the existence of eddy currents and the higher speed above Desk 3, there may be a greater fraction of body deposition with people at Desk 3. There is a vortex above Desk 3 and Desk 1, and the speed above Desk 3 changes rapidly. When there is airflow with pathogenic bacteria in the room, droplets may form on the two

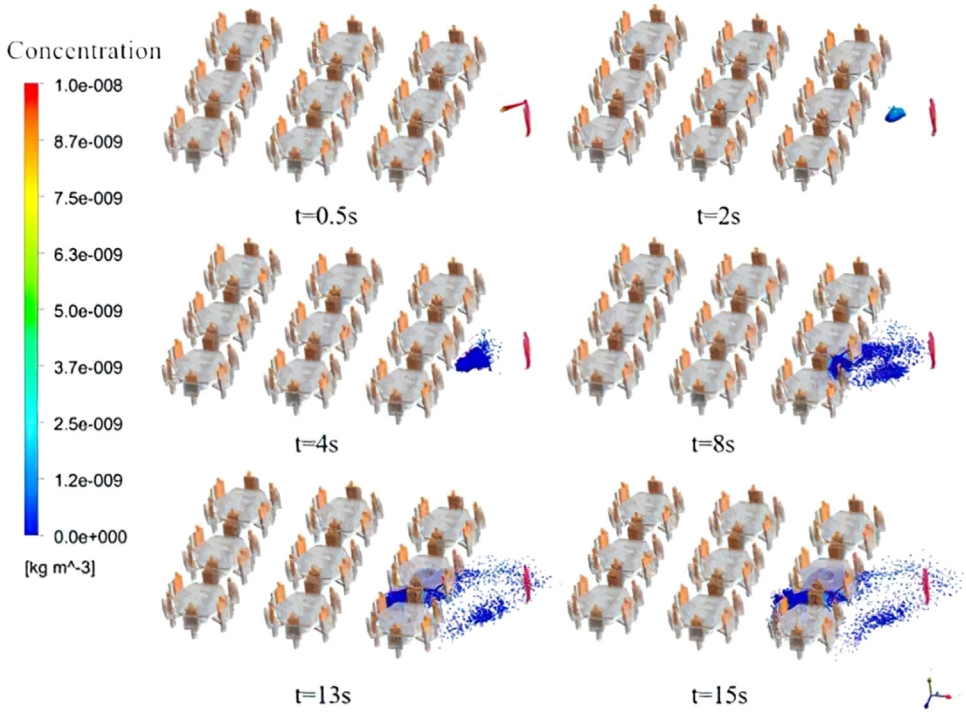

Fig. 6. The spread of droplets at different times when the temperature is 5 °C

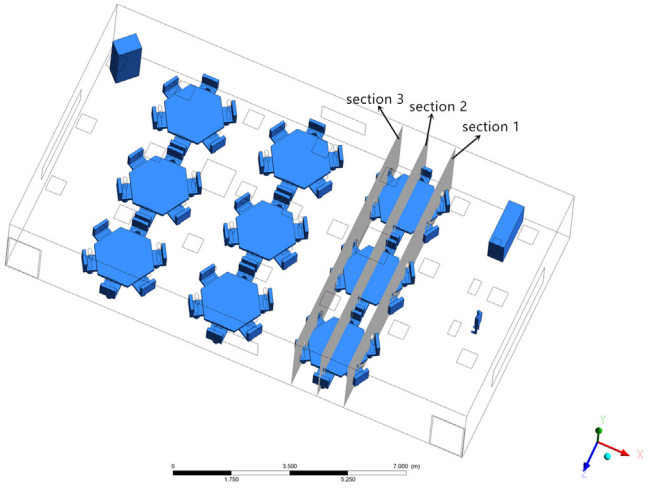

Fig. 7. Selected cross-section diagram

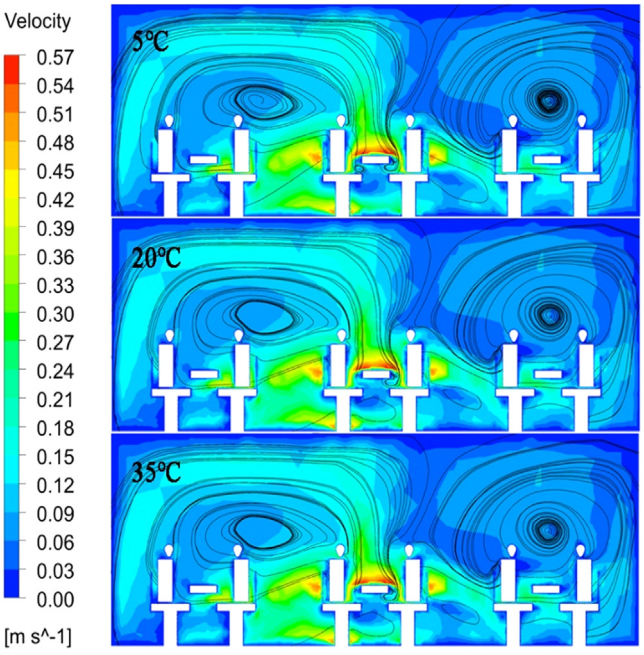

Fig. 8. Velocity and streamline distribution of section 2

desks, which will cause a greater fraction of body deposition with people sitting at the two desks. Comparing the three different temperatures, it can be seen that when the temperature is 5 ˚C, the vortex streamlines are denser and the speed is greater, which corresponds to the increase in the flow rate of droplets due to the decrease in temperature mentioned above.

The spread of droplets is affected by the outdoor temperature, and the low temperature accelerates droplets' speed. When the outdoor temperature is 5 ˚C, droplets' spread faster and reach the wall first, and when the temperature is 20 ˚C, droplets finally reach the wall. Fig. 9 shows the transmission distance of droplets at different times in the X direction and Z direction under different temperatures. The X direction is the same as the initial transmission direction of droplets produced by the human body coughing on the podium, and the Z direction is perpendicular to the initial transmission direction of droplets. It can be seen from Fig. 9(a) that the maximum transmission distance in the X direction at the three temperatures is not much different. This is because the initial velocity of droplets is large, and the air supply velocity of the air conditioner is small. The initial velocity of droplets at the three temperatures is the same, and the air supply temperature is the same, so in the X direction, the transmission distance of droplets at the three temperatures is not much different. It can also be seen from Fig. 9(b) that the distance of droplet transmission at the three temperatures in the first 4 s is the same, but the distance of droplet transmission in the Z direction is significantly different after 4 s.

3.2.2. *Analysis of the body deposition fraction of each desk in the classroom*

It can be seen from the analysis of Fig. 6 that when the classroom is full, and the person on the podium coughs, the body deposition fraction of different desks is evaluated within 15 s: Desk 2 has the highest body deposition fraction, followed by Desk 3. The other desks did not capture droplets within 15 s. According to the statistical data at 15 s, no droplets were arrested on the body of the susceptible human body except the source of infection in the classroom under the three working conditions. Therefore, only the overall body deposition fraction analysis of Desk 2 and Desk 3 is carried out here. According to the definition of body deposition fraction above, droplets deposited on the human body

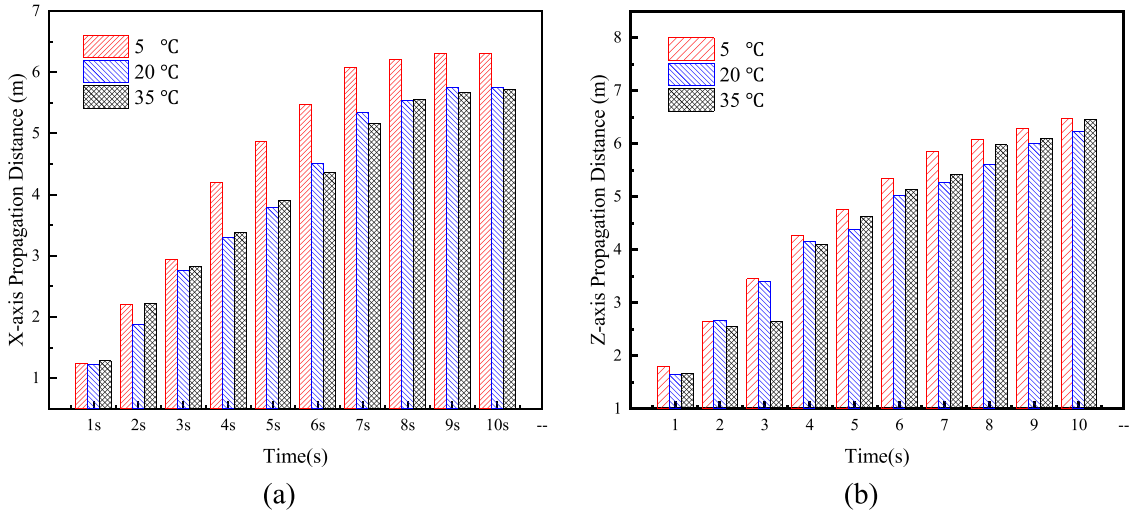

Fig. 9. The propagation distance of droplets in different directions at different moments (a)The propagation distance of droplets on the X-axis at different times, that is, forward propagation (b)The propagation distance of droplets on the Z-axis at different times, that is, the sum of the propagation distances to the left and right

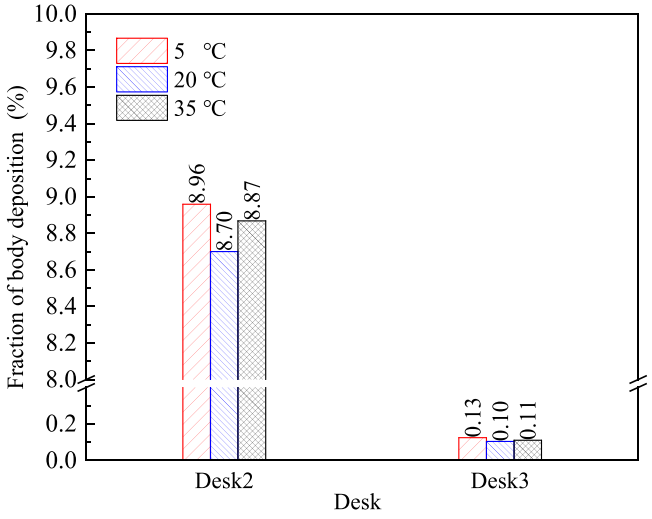

Fig. 10. Body deposition fraction of different desks in scenario

are replaced by droplets deposited on the desk. That is, the body deposition fraction of a certain desk is the ratio of the number of droplets deposited on the desk to the total number of droplets, and the body deposition fraction of the Desk 2 and the third desk are respectively P_2 and P_3. According to the calculation of the statistical results, the body deposition fraction of Desk 2 and Desk 3 under the three working conditions can be obtained as shown in Fig. 10. It can be seen that in the three working conditions, the body deposition fraction of Desk 2 is 72 times that of Desk 3. It is obvious that people sitting at the Desk 2 are more likely to be affected. The reason is that Desk 2 is just in the initial spraying direction of cough droplets from the source of infection, and is the closest distance to the source of infection. At three different temperatures, the body deposition fraction of Desk 2 and Desk is the highest at 5 ˚C, 8.96%, and 0.13%, respectively, followed by 35 ˚C. At 20 ˚C, the body deposition fraction of the two desks is the smallest, 8.70% and 0.11% respectively.

According to the research of the above two scenes, by measuring the average temperature of droplets exhalation height in scene 1 and scene 2, It can be found that the average temperature of droplets exhalation height in scene 2 is 22.72 ˚C, scene 1 is 21.02 ˚C. The average temperature of scene 2 is greater than that of scene 1. Comparing the droplet transmission distance of working condition 2 with that of working condition 1, it can be found that: when the standing teacher coughed, the horizontal transmission distance was 5.66 m, which was 0.93 m longer than that of the seated student. It can be found that the transmission distance of the droplet is affected by the exhalation height of the droplet. The higher droplets' exhalation height, the greater the transmission distance.

4. Conclusion

The method of numerical simulation was used to study the transmission of droplets produced by coughing of the teacher and the student in smart classrooms in different seasons, the influence of outdoor temperature and droplets exhalation height on the spread of droplets caused by coughing of people in the classroom was studied. The body deposition fraction of human bodies other than the source of infection was analyzed, and the following conclusions were drawn:

(1) The low temperature accelerates the transmission speed of droplets. Under the condition that the indoor temperature of the smart classroom is 20 ˚C and the outdoor temperature is 5 ˚C, 20 ˚C, and 35 ˚C respectively, the transmission speed of droplets is the largest at 5 ˚C in 10s. The transmission distance at an outdoor temperature of 5˚C is 9.55% longer than that at 20˚C and 10.31% longer than that at 35˚C. Adjusting the temperature of indoor air conditioners during the epidemic may reduce the spread of droplets effectively.

(2) When the source of infection was a sitting student, the person opposite the source of infection had the greatest fraction of body deposition compared to others in the classroom. The fraction of body deposition in the downwind direction is 6 times higher than that in the upwind direction. When the source of infection is the teacher standing on the podium, the table closest to the source of infection has the highest fraction of body deposition. It is recommended that people in the classroom do not sit face-to-face during the epidemic. The fraction of body deposition between people in the classroom can be reduced by changing the ventilation method and increasing the air outlet.

(3) The transmission distance of droplets is affected by the exhalation height of droplets. When the standing teacher coughed, the horizontal transmission distance was 5.66 m, which is 0.93 m longer than the sitting student. Therefore, on the basis of ensuring normal teaching, the exhalation height of droplets should be reduced as much as possible. For example, on the basis of satisfying ergonomics, the height of chairs and podiums in smart classrooms should be reduced as much as possible.

Declaration of Competing Interest

The authors declare that they have no known competing financial interests or personal relationships that could have appeared to influence the work reported in this paper.

Acknowledgments

The study is supported by Hubei Technological Innovation Special Fund (Grant Nos. 2020ZYYD019)

Supplementary materials

Supplementary material associated with this article can be found, in the online version, at doi:10.1016/j.heha.2022.100015.

References

Abdi, D.S., Bitsuamlak, G.T., 2014. Wind flow simulations on idealized and real complex terrain using various turbulence models. Adv. Eng. Softw. 75, 30–41. doi:10.1016/j.advengsoft.2014.05.002, 2014.

Cai, Y., 2019. Study on the propagation characteristics of respiratory droplet aerosol pollutants in the car compartment[D]. Shenyang Architectural University doi:10.27809/d.cnki.gsjgc.2019.000423.

Carrillo, C.C., Rodríguez, S.S.J., Aranaga, I.L., et al., 2019. Diagnostic delay as main contributing factor to a large outbreak of tuberculosis in a university. Enferm. Infec. Microbiol. Clin (English ed.) 37 (8), 496–501. doi:10.1016/j.eimce.2019.04.009.

Chao, CY., Wan, MP., 2006. A study of the dispersion of expiratory aerosols in unidirectional downward and ceiling-return type airflows using a multiphase approach. Indoor air 16 (4), 296–312. doi:10.1111/j.1600-0668.2006.00426.x.

Chen, C., Zhao, B., 2010. Some questions on dispersion of human exhaled droplets in ventilation room: answers from numerical investigation. Indoor Air 20, 95–111. doi:10.1111/j.1600-0668.2009.00626.x.

Cao, G., Nielsen, P.V., Jensen, R.L., Heiselberg, P., Liu, L., Heikkinen, J., 2015. Protected zone ventilation and reduced personal exposure to airborne cross infection. Indoor Air 25, 307–319. doi:10.1111/ina.12142.

Deacon, J., 2001. The Microbial World—Airborne microorganisms. Institute of Cell and Molecular Biology, and Biology Teaching Organisation, University of Edinburgh.

Disease outbreaks. 2020a. World Health Organization. https://www.who.int/emergencies/diseases/en/ accessed 5 February 2020.

Gao, F., 2014. Study on airborne infection control strategy of pulmonary tuberculosis based on upper chamber ULTRAVIOLET radiation technology[D]. Huazhong University of Science and Technology doi:10.7666/d.D614299.

Gao, N., Niu, J., Morawska, L., 2010. Distribution characteristics of human exhaled aerosols in a closed environment. Journal of Southeast University (English Edition) 26 (02), 232–237. doi:10.3969/j.issn.1003-7985.2010.02.019.

Hang, J., Li, Y., Jin, R., 2014. The influence of human walking on the flow and airborne transmission in a six-bed isolation room: Tracer gas simulation. Build Environ 77, 119–134. doi:10.1016/j.buildenv.2014.03.029.

He, Q., Niu, J., Gao, N., Zhu, T., Wu, J., 2011. CFD study of exhaled droplet transmission between occupants under different ventilation strategies in a typical office room. Build Environ 46 (2), 397–408. doi:10.1016/j.buildenv.2010.08.003.

Health Commission website, 2022. Notice on Printing and Distributing the Novel Coronavirus Pneumonia Diagnosis and Treatment Plan (Ninth Trial Version).

Kang, Z., Zhang, Y., Fan, H., Feng, G., 2015. Numerical Simulation of Coughed Droplets in the Air-Conditioning Room[C]. Procedia Engineering 121, 114–121. doi:10.1016/j.proeng.2015.08.1031.

Kang, Z., Zhang, Y., Feng, G., et al., 2017. Numerical Simulation of Droplet Aerosols in Conference Room. Journal of Shenyang Jianzhu University (Natural ence) 33 (3), 562–568. doi:10.11717/j.issn:2095-1922.2017.03.22.

Li, X., Shang, Y., Yan, Y., Yang, L., Tu, J., 2018. Modelling of evaporation of cough droplets in inhomogeneous humidity fields using the multi-component Eulerian-Lagrangian approach. Build Environ 128, 68–76. doi:10.1016/j.buildenv.2017.11.025.

Liu, S., 2007. Research on the indoor propagation and movement of microbial aerosols emitted by oral cavity[D]. Tianjin University doi:10.7666/d.y1362506.

Liu, X., Huang, J., Li, C., et al., 2021. The role of seasonality in the spread of COVID-19 pandemic. Environ. Res. 195, 110874. doi:10.1016/j.envres.2021.110874.

Liu, P., Zhang, H., Dan, L., 2016. Dynamic properties of indoor propagation of human droplets[J]. Refrigeration and Air Conditioning (Sichuan) 30 (4), 371–376. doi:10.3969/j.issn.1671-6612.2016.04.001.

Nicas, M., Best, D., 2008. A Study Quantifying the Hand-to-Face Contact Rate and Its Potential Application to Predicting Respiratory Tract Infection. J OCCUP ENVIRON HYG 5, 347–352. doi:10.1080/15459620802003896.

Notice on the issuance of COVID-19 Protocol. Revised eighth trial edition. 2021. National Health Commission of the People's Republic of China. http://www.nhc.gov.cn/yzygj/s7653p/202104/7de0b3837c8b4606a0594aeb0105232b.shtml accessed 4 October 2021.

Novel Coronavirus (2019-nCoV) situation reports. 2020b. World Health Organization. https://www.who.int/emergencies/diseases/novel-coronavirus-2019/situation-reports/ accessed 5 February 2020.

Ong, S.W.X., Tan, Y.K., Chia, P.Y., Lee, T.H., Ng, O.T., Wong, M.S.Y., Marimuthu, K., 2020. Air, Surface Environmental, and Personal Protective Equipment Contamination by Severe Acute Respiratory Syndrome Coronavirus 2 (SARS-CoV-2) From a Symptomatic Patient. JAMA 323 (16), 1610–1612. doi:10.1001/jama.2020.3227.

Rahimi, A., Tavakoli, T., Zahiri, S., 2014. Computational Fluid Dynamics (CFD) Modeling of Gaseous Pollutants Dispersion in Low Wind Speed Condition: Isfahan Refinery, a Case Study. Pet Sci Technol 32 (11), 1318–1326. doi:10.1080/10916466.2011.653701.

Sun, N., Huang, Y., Zhang, R., 2020. Survival time of 2019 novel coronavirus in different environment and its significance in the protection of clinical areas in otolaryngology department[J]. Chinese Journal of Ophthalmology and otorhinolaryngology 20 (3), 258–260. doi:10.14166/j.issn.1671-2420.2020.03.034.

Wang, J., Yao, Y., 2020. Research on the Construction Status and Application Strategies of Smarter Classrooms in Colleges and Universities. Software 41 (6), 261–266. doi:10.3969/j.issn.1003-6970.2020.06.054.

Wang, X., Ren, A., Wu, Y., Wang, B., Shi, L., He, Y., 2020. Numerical simulation of cough droplets transmission based on Euler-Lagrange method[J]. Nature 42 (3), 239–248. doi:10.3969/j.issn.0253-9608.2020.03.009.

Wang, F., 2004. Computational Fluid Dynamics Analysis[M]. Tsinghua University Press, Beijing, pp. 24–26.

Wang, J., 2011. Simulation of the evaporation and dispersion process of exhaled droplets[D]. Jiangsu: Southeast University doi:10.7666/d.Y1977397.

Wang, R., Zhang, K., Wang, G., 2007. Fluent technology foundation and application examples[M]. Tsinghua University Press, Beijing, pp. 134–136.

Wei, L., 2007. Numerical simulation and experimental study of indoor air flow organization of variable air volume air conditioning system in intelligent buildings[D]. Beijing Institute of Civil Engineering and Architecture.

Yang, X., Ou, C., Yang, H., Liu, L., Song, T., Kang, M., Lin, H, Hang, J., 2020. Transmission of pathogen-laden expiratory droplets in a coach bus[J]. J. Hazard. Mater. 397, 122609. doi:10.1016/j.jhazmat.2020.122609.

Yang, C., Yang, X, Zhao, B., 2016. Person to person droplets transmission characteristics in unidirectional ventilated protective isolation room: The impact of initial droplet size. Build Simul 9, 597–606. doi:10.1007/s12273-016-0290-7.

Yu, H., Zhang, Y., Chen, X., He, G., Sun, F., Li, Y., Chen, J, Zhang, W., 2020. Whole-genome sequencing and epidemiological analysis of a tuberculosis outbreak in a high school of southern China. Infect. Genet. Evol 83, 104343. doi:10.1016/j.meegid.2020.104343.

Zhang, Y., Feng, G., Kang, Z., Bi, Y., Cai, Y., 2017. Numerical Simulation of Coughed Droplets in Conference Room[C]. Procedia Engineering 205, 302–308. doi:10.1016/j.proeng.2017.09.981.

Zhang, Y., Feng, G., Bi, Y., Cai, Y., Zhang, Z., Cao, G., 2019. Distribution of droplet aerosols generated by mouth coughing and nose breathing in an air-conditioned room. Sustain. Cities. Soc. 51, 101721. doi:10.1016/j.scs.2019.101721.

Zhang, X., 2011. Numerical simulation of the propagation process of infectious droplets in the air[D]. Inner Mongolia: Inner Mongolia University of Science and Technology doi:10.7666/d.D292131.

Zhao, X., 2006. Experimental research on the movement and spread of indoor biological particles[D]. Tianjin University.

Zhao, B., Zhang, Z., Li, X., 2003. A numerical study of the spread of human droplets in the room. HVAC (3) 176–178.

Zhu, S., Kato, S., Yang, J-H., 2006. Study on transport characteristics of saliva droplets produced by coughing in a calm indoor environment. Build Environ[J] 41 (12), 1691–1702. doi:10.1016/j.buildenv.2005.06.024.